

Provided for non-commercial research and educational use only.
Not for reproduction or distribution or commercial use.



This article was originally published in a journal published by Elsevier, and the attached copy is provided by Elsevier for the author's benefit and for the benefit of the author's institution, for non-commercial research and educational use including without limitation use in instruction at your institution, sending it to specific colleagues that you know, and providing a copy to your institution's administrator.

All other uses, reproduction and distribution, including without limitation commercial reprints, selling or licensing copies or access, or posting on open internet sites, your personal or institution's website or repository, are prohibited. For exceptions, permission may be sought for such use through Elsevier's permissions site at:

<http://www.elsevier.com/locate/permissionusematerial>



ELSEVIER

Available online at www.sciencedirect.com

ScienceDirect

Comparative Biochemistry and Physiology, Part A 145 (2006) 533–539

CBP

www.elsevier.com/locate/cbpa

In vitro estimates of power output by epaxial muscle during feeding in largemouth bass

David J. Coughlin^{a,*}, Andrew M. Carroll^b

^a Department of Biology Widener University Chester, PA 19013, USA

^b Department of Organismic and Evolutionary Biology Harvard University Cambridge, MA 02138, USA

Received 22 June 2006; received in revised form 24 August 2006; accepted 25 August 2006

Available online 30 August 2006

Abstract

Recent work has employed video and sonometric analysis combined with hydrodynamic modeling to estimate power output by the feeding musculature of largemouth bass in feeding trials. The result was an estimate of $\sim 69 \text{ W kg}^{-1}$ of power by the epaxial muscle during maximal feeding strikes. The present study employed *in vitro* measurements of force, work and power output by fast-twitch epaxial muscle bundles stimulated under activation conditions measured *in vivo* to evaluate the power output results of the feeding experiments. Isolated muscle bundles from the epaxial muscle, the sternohyoideus and the lateral red or slow-twitch muscle were tied into a muscle mechanics apparatus, and contractile properties during tetanic contractions and maximum shortening velocity (V_{\max}) were determined. For the epaxial muscles, work and power output during feeding events was determined by employing mean stimulation conditions derived from a select set of maximal feeding trials: 17% muscle shortening at 3.6 muscle lengths/s, with activation occurring 5 ms before the onset of shortening. Epaxial and sternohyoideus muscle displayed similar contractile properties, and both were considerably faster ($V_{\max} \approx 11\text{--}13 \text{ ML s}^{-1}$) than red muscle ($V_{\max} \approx 5 \text{ ML s}^{-1}$). Epaxial muscle stimulated under *in vivo* activation conditions generated $\sim 60 \text{ W kg}^{-1}$ with a 17% strain and $\sim 86 \text{ W kg}^{-1}$ with a 12% strain. These values are close to those estimated by hydrodynamic modeling. The short lag time (5 ms) between muscle activation and muscle shortening is apparently a limiting parameter during feeding strikes, with maximum power found at an offset of 15–20 ms. Further, feeding strikes employing a faster shortening velocity generated significantly higher power output. Power production during feeding strikes appears to be limited by the need for fast onset of movement and the hydrodynamic resistance to buccal expansion.

© 2006 Elsevier Inc. All rights reserved.

Keywords: Epaxial muscle; Muscle mechanics; Hydrodynamic modeling; Shortening velocity; Sternohyoideus; Suction feeding; Sunfish

1. Introduction

Suction feeding is one of the most ubiquitous behaviors among vertebrates and is common to most species of teleost fish, as well as many anamniotic vertebrates, marine mammals, and aquatic reptiles (Lauder, 1980; Ferry-Graham and Lauder, 2001). Therefore, understanding how muscles function during suction feeding may yield insights into the physiology, ecology, and evolution of numerous vertebrate lineages (i.e., Ferry-Graham et al., 2002; Westneat, 2004). While it has been relatively straightforward to measure muscle activation and

strain during suction feeding with either sonomicrometry or X-ray ciné along with electromyography (Carroll, 2004; Van Wassenbergh et al., 2005), muscle force has been more difficult to estimate. In this study the force produced by isolated bundles of feeding muscle was measured during imposed activation and strain cycles similar to those observed during suction feeding, as has been used routinely in studies of fish swimming muscle function (e.g., Rome et al., 1993; Coughlin, 2000; Syme and Shadwick, 2002).

These force measurements enabled estimations of cycle muscle power which could be used to validate previous *in vivo* work on suction feeding muscle function. First, estimates of muscle power during realistic activation and strain regimes (derived from literature) were compared to that measured *in vivo* to validate those results. Second, activation and strain were

* Corresponding author. Tel.: +1 6104994025; fax: +1 6104994496.

E-mail address: coughlin@pop1.science.widener.edu (D.J. Coughlin).

varied to elicit maximal power from these bundles. These *optimal* conditions could be compared to those found *in vivo* to understand how the mechanical and behavioral demands of suction feeding may influence suction feeding performance.

During suction feeding in fish, a predator rapidly expands its cranial skeleton to create a flow of water into the mouth which captures the prey item. To capture elusive prey this flow, and the cranial kinematics creating it, must be rapid enough to prevent the prey from escaping entrainment. These rapid kinematics in a dense fluid medium impose loads on skeletal elements (Lauder, 1980; Lauder and Lanyon, 1980) and the muscles actuating their movement (Van Wassenbergh et al., 2005). This loading is predominantly due to high sub-ambient pressures (-5 to -25 kPa for *Micropterus salmoides*) inside the oral cavity and is distinct from more well-studied accelerative or drag-based loading (e.g., Roberts and Marsh, 2003; Reilley et al., 2005). Expansion during suction feeding is due to contraction of the dorsal epaxial musculature and ventral sternohyoideus and hypaxial musculature which rotate the neurocranium away from the buccal floor and (through more complex linkages) actuate jaw opening and lateral cranial expansion. Therefore, both sternohyoideus and epaxial fibers were used in this study.

Muscle power output during suction feeding has recently been estimated by Carroll and Wainwright (2006) using direct measurements of intra-oral pressure and muscle strain. These results were consistent with early hydrodynamic estimates (de Jong et al., 1987). The kinematic movement and fluid loading required for suction feeding has a profound effect on muscle performance. First, because loads are developed due to movement, the muscle is not prevented from shortening prior to full activation, potentially limiting peak stress. Second, to actuate large skeletal displacement, muscle fascicles shortened by $>20\%$ strain during high performance strikes, potentially resulting in muscle sarcomeres operating off of the peak of the sarcomere-length–tension plateau. Both of these suggestions differ from previous studies of muscle systems that function for high instantaneous power production. For instance, during jumping frog muscle is maximally activated prior to shortening and operates at low enough strains such that force production is high throughout the jump (Lutz and Rome, 1996a,b). If the *optimal* conditions found in this study differ from those found *in vivo*, it would suggest that the mechanical and behavioral requirements of suction feeding, in fact, limit suction feeding power production and, thus, performance. This potentially represents an example of suboptimal *in vivo* muscle function due to behavioral constraints. The present study was undertaken to contribute a third estimate of power output by a feeding muscle and to examine constraints on muscle performance during suction feeding events in bass.

While the musculoskeletal system may not be able to overcome certain constraints to allow maximal power productions, given a certain load, the gearing of the skeletal system may be such that loads allow muscles to shorten at or near *optimal* contraction velocities (Rome et al., 1988). Based on shortening data in the sternohyoideus, Carroll (2004) suggested that largemouth bass were geared for maximal power production. However, absent *in vitro* data on the specific

relationship between power production and strain rate in this animal these statements remain conjectural. This study was undertaken with three goals: (1) to compare levels of power measured in this study under realistic strain regimes with those measured *in vivo*, (2) to compare optimal *in vitro* strain rates for power production with those measured *in vivo* two other studies (e.g., Carroll and Wainwright, 2006), and (3) to compare levels of power under *optimal* conditions with that measured *in vivo*. Prior to experiments measuring power production by epaxial muscle under *in vivo* muscle activity conditions, the contractile properties of epaxial muscle were measured. In addition, the contractile properties of the sternohyoideus muscle, another presumably fast-twitch feeding muscle, and myotomal, slow-twitch red muscle were characterized for comparison.

2. Materials and methods

2.1. Animals

Largemouth bass (*M. salmoides*) were obtained from Kurtz Fish Farm, Chester County, PA. The fish were maintained in a re-circulating aquaria at 25 °C and fed live fish. Data are reported here for nine fish (Mean \pm S.D.: mass, 420 ± 135 g; TL, 29.9 ± 5.0 cm; SL 26.8 ± 4.6 cm). All handling of experimental animals was reviewed by the Widener University Institutional Animal Care and Use Committee in accordance with the Guide for the Care and Use of Laboratory Animals of the National Research Council.

2.2. Physiology experiments

Epaxial, sternohyoideus and red axial muscle bundles were used to examine contractile properties. To perform mechanics experiments, the fish were killed by spinal transection and pithing. For all three muscle types, the scales were removed and strips of muscles (~ 1.0 mm wide) were extracted. Red muscle was extracted from the lateral myotome just above and below the lateral line at a position of 0.60 TL from the snout. Epaxial muscle was extracted from a mid-dorsal position within 2 cm of the caudal margin of the neurocranium. Sternohyoideus muscle was extracted from a mid-ventral position just in front of the pelvic girdle. Subsequent dissection was carried out in physiological saline at 4 °C with the use of stereomicroscope (Coughlin et al., 2005). Live muscle bundles were the length of one myomere (~ 7 – 9 mm in epaxial muscle bundles, ~ 6 – 7 mm for sternohyoideus bundles and ~ 4 – 5 mm red muscle) with a live muscle fibre cross-sectional area of 0.25 – 1.0 mm². Using a muscle mechanics system comprised of a servomotor (Cambridge Technology 300S) and a force transducer (Cambridge Technology 404A), the muscle bundles were tied into the system and maintained at a temperature of 25 °C for all experiments. The physiological saline was aerated gently to supply oxygen and to induce circulation. Experimental control (i.e., stimulation patterns and length change ramps) and data collection (force level and muscle length) were carried out using a National Instruments A/D board and custom LabView software routines.

Activation conditions (muscle length, pulse length and amplitude for twitch contractions, stimulus duration and frequency tetanic contractions) for each bundle were optimised to generate the maximal tetanic force. The duration of the stimulus was 200–250 ms for red muscle and 100–125 ms for epaxial and sternohyoideus muscle. The stimulus was composed of 1–2 ms pulses at a frequency of 200–400 Hz. The amplitude of each pulse was typically 7–9 V. For tetanic contractions, time of activation (TA) was defined as the time from 10% to 90% of maximum isometric stress. Time of relaxation (TR) was the time from 90% to 10% of peak isometric stress. Twitch time (TW 90) was defined as the time from stimulation to 90% recovery (10% of peak isometric stress) in twitch contractions. Maximum shortening velocity (V_{\max}) was determined for each muscle bundle by imposing a series of isovelocity ramps once the ramp had reached maximal force during isometric activation. Force–velocity curves could then be plotted from each velocity versus the corresponding resulting force level. V_{\max} was estimated using the Hill equation. Maximum steady-state or instantaneous power (W_{\max}) at the corresponding optimal shortening velocity (V_{opt}) was calculated by plotting the power (=force * velocity) versus velocity curve. W_{\max} is the peak of the power versus velocity curve. V_{opt} is the corresponding velocity at which power is maximized.

For epaxial muscle, *in vitro* estimates of power production during feeding events were made by imposing experimental velocity ramps on bundles. The values used for the amplitude and velocity of the experimental ramps and the timing of muscle activation relative to shortening were based on *in vivo* measurements of muscle activity. Carroll and Wainwright (2006) reported on epaxial muscle activity during feeding strikes (Fig. 1). Based on seven maximal strikes, mean values of shortening amplitude (17%), shortening velocity (3.6 muscle lengths per second (ML s^{-1})) and onset of muscle activation (5 ms prior to shortening). Power output during shortening was then determined for both 17% shortening and for 12% of shortening. These values are referred to below as the “standard conditions”. Additional experimental velocity ramps were carried out across a range muscle activation (0–30 ms prior to shortening) and shortening velocities (1.6–6.6 ML s^{-1}). Power was calculated as the area under the curve of force versus length change during the entire shortening period (12% or 17%, see Fig. 5) divided by the time of shortening. Since force is not constant throughout shortening, power output reported for the experimental velocity ramps represents an estimate of an average value of power during a feeding strike. This is equivalent to the approach of Carroll and Wainwright (2006). They used pressure levels in the buccal cavity to estimate force levels. By combining their estimated force with muscle shortening during feeding strikes, they reported “average” levels of power by the epaxial muscle during suction feeding strikes.

In the present study, we also reanalyzed the experimental velocity ramp experiments to determine peak instantaneous power during simulated feeding strikes. Peak power was defined as the power produced during the experimental velocity ramp

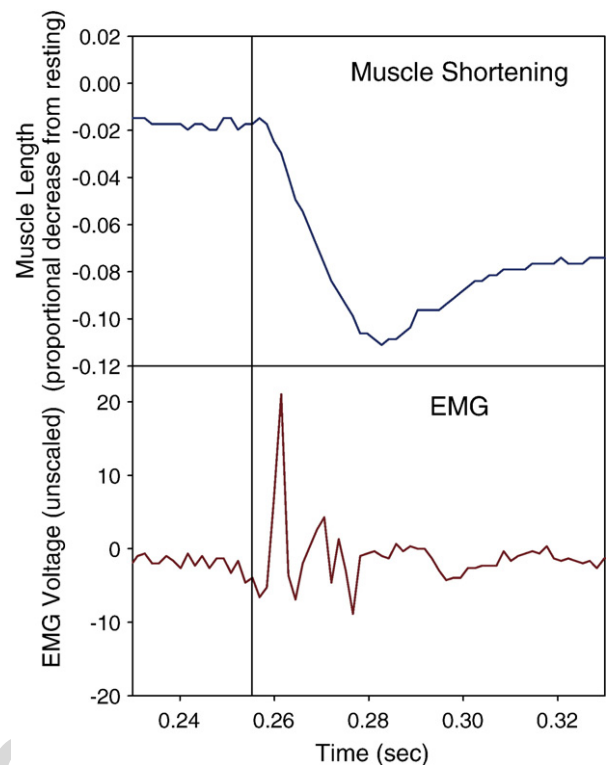


Fig. 1. Sample *in vivo* recording of a prey strike by a largemouth bass. Muscle activation occurred ~5 ms prior to the onset of shortening and continued throughout the shortening period. Muscle shortened by ~11% at a rate of 3.5 ML s^{-1} . The data are from Carroll and Wainwright (2006).

when force is within 10% of the peak force of a given velocity ramp trial. Peak power levels were calculated as above—the area under the portion of the force vs. length change divided by the time of shortening.

2.3. Histological analysis

At the end of each experiment, the fibre area of the live muscle bundles was determined histologically. The bundles were initially stained for one hour in trypan blue dissolved in physiological saline. Then, muscle bundles were embedded in gelatin (15% in physiological saline) and frozen in liquid nitrogen. Frozen bundles were sectioned at 16 μm using a CryoStat. Sections were mounted on slides and stained for succinic dehydrogenase (SDH) for mitochondrial content. In cross-sections of muscle bundles, dead muscle fibres appeared blue, aerobic muscle fibres were dark brown and anaerobic muscle fibres were light brown. The cross-section of live muscle fibres within the experimental muscle bundles could be determined by excluding both dead fibres and connective tissue. The proportion of muscle fibre relative to total live muscle (i.e., muscle fibre and connective tissue) was determined empirically for an epaxial muscle bundle as 0.770 and for a sternohyoideus bundle as 0.788. Initial estimates of force production by epaxial muscle substantially underestimated true force until these correction factors were employed. For red muscle, a correction factor of 0.7 was used based on previous work (Coughlin, 2000). The final live muscle fibre cross-sectional area was used

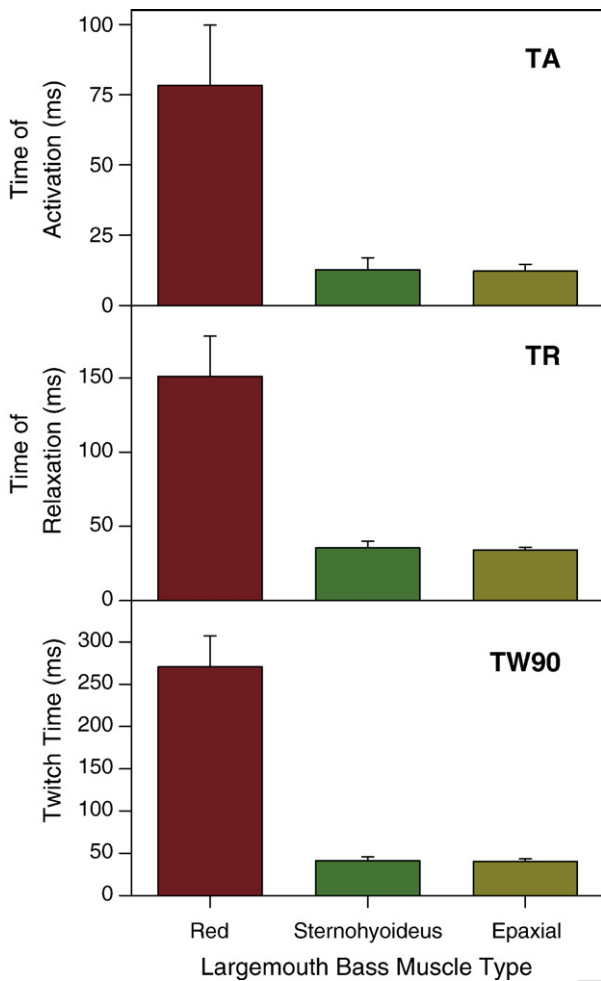


Fig. 2. Isometric contractile properties of bass muscle. The two feeding muscles, epaxial and sternohyoideus, displayed significantly faster activation (TA), relaxation (TR) and twitch times (TW90) relative to red muscle. Statistical results given in the text.

to calculate isometric tension for twitch and tetanic contractions. Tension (force per unit area) calculated from measures of force production and the estimated live muscle bundle area ranged from $\sim 100 \text{ kN m}^{-2}$ for epaxial and sternohyoideus muscle and $100\text{--}150 \text{ kN m}^{-2}$ for red muscle.

2.4. Statistical analysis

ANOVA was used to determine if there were differences in contractile properties among muscle fiber types tested here. Tukey post hoc comparisons were used to determine which fiber types differed given a significant ANOVA result for any given contractile property. The contractile properties were analyzed for the effects of muscle fiber type were TA, TR, TW 90, V_{\max} , V_{opt}/V_{\max} and W_{\max} .

Power production during experimental velocity ramps was also analyzed via ANOVA. Power output of muscle bundles stimulated under experimental velocity ramps was the dependent variable. In the experiment in which the timing of muscle activation was varied, ANOVA was used to test for the effect of individual muscle bundle (random effects variable), timing of

muscle activation (fixed variable, 0–30 ms) and the total muscle shortening (fixed variable, 12 vs. 17%) on power output. In the experiment in which experimental ramp velocity was varied, ANOVA was used to test for the effect of individual muscle bundle (random effects variable) and ramp velocity (fixed variable) on power output. SPSS was used for all statistical tests.

3. Results

In isometric contractions, the epaxial and sternohyoideus muscles were indistinguishable and both displayed significantly faster contractile properties than red muscle. The fast-twitch muscle displayed relatively fast contractile properties, red muscle taking six times longer to activate, four times longer to relax and close to seven times longer for total twitch time (Fig. 2). Fiber type had a significant effect on all three isometric variables (ANOVA; TA, $F=8.2$, $p=0.004$; TR, $F=16.5$, $p=0.0002$; TW90, $F=43.3$, $p<0.0001$; $df=2,14$). In post hoc

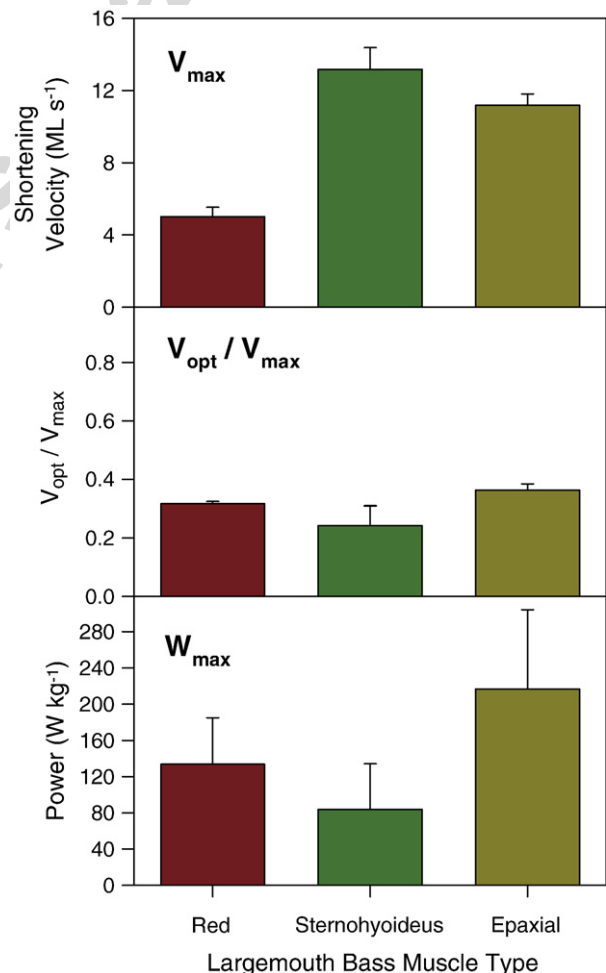


Fig. 3. Contractile properties derived from isotonic contractions. Epaxial and sternohyoideus muscles had significantly faster maximum shortening velocities (V_{\max}) compared to red muscle. There was modest but significant variation in the ratio of optimal shortening velocity (V_{opt} , where power is maximal) to V_{\max} . The sternohyoideus had a significantly lower V_{opt}/V_{\max} ratio. In terms of power production at V_{opt} , epaxial muscle produced significantly more power than red or sternohyoideus muscle. Statistical results given in the text.

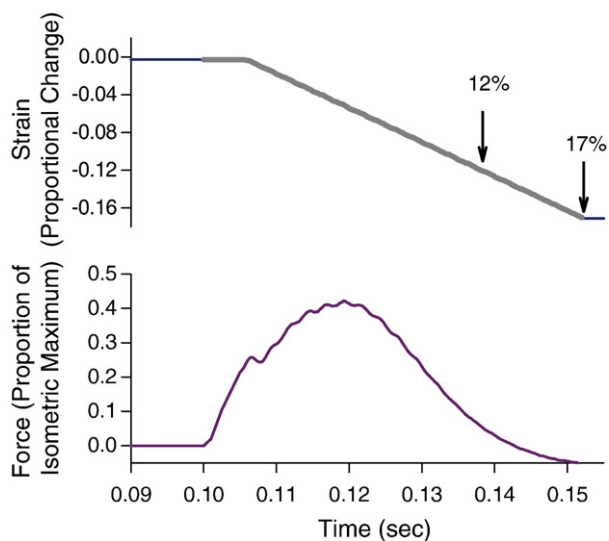


Fig. 4. Sample velocity ramp representing a simulated feeding strike. Under the “standard conditions” based on seven maximal feeding strikes recorded by Carroll and Wainwright (2006), epaxial muscle bundles were shortened 5 ms after being stimulated. Shortening was 3.6 ML s^{-1} for a total of 17% of resting length. The thick region on the upper trace represents the period of stimulation. Force production peaks 20 ms after the onset of stimulation and 15 ms after the beginning of shortening. Force level drops to near zero after shortening by 12%.

tests, the epaxial and sternohyoideus muscle did not differ from each other for any of the variables (Tukey test, $p > 0.05$ for TA, TR and TW90).

Based on measurements from isotonic contractions, the epaxial and sternohyoideus muscles again could not be distinguished based on V_{\max} . The red muscle V_{\max} was less than half that of the fast-twitch fiber types (Fig. 3). Fiber type had a significant effect on V_{\max} (ANOVA; $F = 32.7$, $p < 0.0001$; $df = 2, 14$), but epaxial and sternohyoideus muscles were not statistically different from one another (Tukey–Kramer test, $p > 0.05$). V_{opt} , when expressed as a proportion of V_{\max} , also varied with fiber type (ANOVA; $F = 5.03$, $p = 0.022$; $df = 2, 14$), with epaxial muscle having the highest V_{opt}/V_{\max} ratio and sternohyoideus having the lowest (Tukey test, $p < 0.05$). Lastly, maximum steady state power output did appear to vary considerably between fiber types (Fig. 3). However, this effect was not statistically significant (ANOVA; $F = 0.73$, $p = 0.50$; $df = 2, 14$). The relatively high level of variability in this variable means that acceptance of the null hypothesis is done with relatively low power (Power < 0.30).

When isolated muscle bundles were activated under the experimental velocity ramps employing the “standard conditions”, force initially increased rapidly during the 5 ms between onset of activation and the onset of shortening. Force dipped at the onset of shortening but then continued to rise, reaching about 50% of peak isometric force after approximately 15 ms of shortening. After that point, force decayed rapidly, typically reaching zero active force produced after shortening by about 12% (Fig. 4). Beyond the 12% strain, force levels were typically negative, meaning force was applied to shorten the muscle. When plotted as force versus length, the results of experimental velocity ramps under the “standard conditions” reflect much

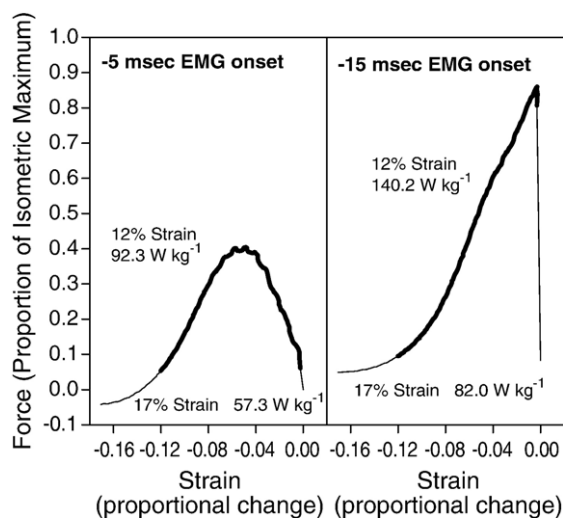


Fig. 5. Force plotted against length change for two simulated feeding strikes, one under the “standard conditions” (left panel) and one with a longer lag between onset of muscle activation and the onset of muscle shortening (right panel). The period of shortening up to 12% is indicated by the thicker line, with a “tail” of low force during shortening until 17% strain. Power output was determined as the area under the curve for force times shortening velocity. Power output was much higher when only 12% shortening was analyzed versus the full 17%. Further, increasing the lag time between muscle activation and shortening substantially increases power output. With 15 ms lag between muscle activation and shortening, the muscle reaches near peak tetanic force prior to shortening.

lower power output relative to the steady state maximum due in large part to the force levels being less than half of the peak isometric force. Power output of experimental velocity ramps is substantially higher when analysis is limited a total shortening length of 12% instead of the full 17% of the standard conditions (Fig. 5). Increasing the lag between the onset of activation and the onset of shortening also substantially increases power output. With a lag of 15 ms, force levels reach 80–90% of the isometric maximum before shortening in these ramps, resulting in a 50% increase in power output for ramps analyzed at 12% or

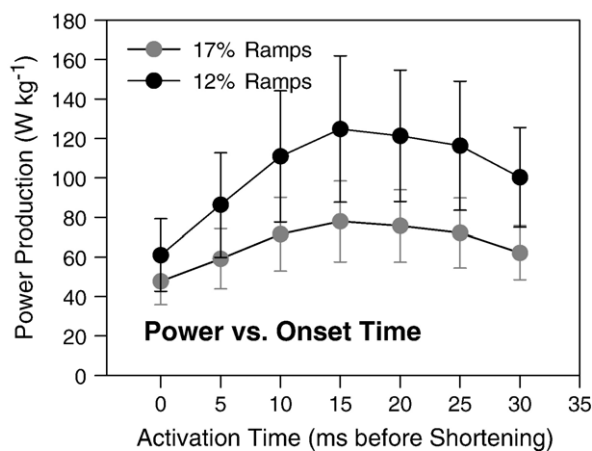


Fig. 6. Power production as a function of activation time. Power output during simulated feeding strikes peaks with a lag time of 15 ms between muscle activation and shortening for analysis of both the 12% and 17% strain. The power produced under the shorter strain was significantly higher than under the longer strain.

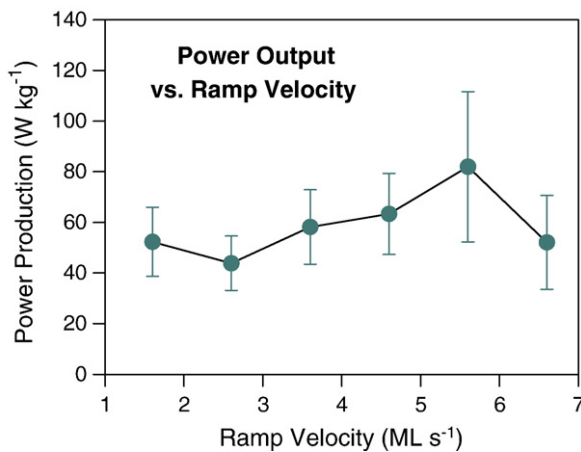


Fig. 7. Power production as a function of ramp velocity. Power output during simulated feeding strikes peaks at a shortening velocity of 5–6 ML s⁻¹. All muscle bundles display a minimum power output at 2.6 ML s⁻¹, with slightly more power observed at 1.6 ML s⁻¹.

17% shortening amplitude. The 15 ms lag in activation represented the peak condition for power output (Fig. 6). The timing of muscle activation relative to muscle shortening, the strain level and individual muscle bundle all had significant effects on power output (ANOVA; muscle onset, $F=13.4$, $p=0.004$, $df=7,5.6$; strain, $F=7.72$, $p=0.039$, $df=1,5.0$; individual bundle, $F=10.9$, $p=0.005$, $df=5,6.1$).

Reanalyzing the experimental velocity ramp data to determine peak power levels for each experimental velocity ramp resulted in substantially higher power levels than the average power levels for the full length ramp. For instance, under the standard conditions, muscle bundles produced an average of 59 W kg⁻¹ for 17% strain and 86 W kg⁻¹ for 12% strain (Fig. 6), while the peak power during those ramps was ~124 W kg⁻¹. For the experimental velocity ramps employing 15 ms lag between activation and muscle shortening, muscle bundles produced 77 W kg⁻¹ for 17% strain and 124 W kg⁻¹ for 12% strain (Fig. 6) but had a peak power output of 168 W kg⁻¹.

Increasing ramp velocity of experimental velocity ramps resulted in an increase in power production (Fig. 7). Ramp velocity and individual muscle bundle both had significant effects on power output (ANOVA; velocity, $F=12.8$, $p=0.005$, $df=6,5.42$; individual bundle, $F=81.4$, $p<0.001$, $df=5,17$). Note that the non-integer degrees of freedom result from tests involving unbalanced cells.

4. Discussion

4.1. Comparison with other teleost muscles

The epaxial muscle of largemouth bass displays the characteristics of a fast-twitch muscle. Its contractile properties, as reported here for data at 25 °C, are much faster than slow-twitch red muscle and similar to published values of fish white muscle properties. For instance, Wakeling and Johnston (1998) reported maximum shortening velocity in the rostral swimming muscle from a scorpionfish, *Scorpaena notata*, of 13.2 ML s⁻¹

at 20 °C. Other reported values for maximum shortening velocity of fish white muscle are at lower temperatures. For example, the rostral white myotome (swimming muscle) sculpin, *Myoxocephalus scorpius*, has a V_{max} of 7.6 ML s⁻¹ at 12 °C (James et al., 1998), and the rostral white myotome in cod, *Gadus morhua*, has a V_{max} values of 6.9 ML s⁻¹ at 5 °C (Davies et al., 1995). The activation and relaxation times of bass muscle are comparable to these species as well. Activation in bass epaxial muscle is slightly faster than the white muscle of scorpionfish and much faster than the sculpin at the colder temperature. However, the maximum isometric tension of bass epaxial muscle (~100 kN m⁻²) is considerably less than that reported for these other fishes (e.g., ~240 kN m⁻² for scorpionfish, Wakeling and Johnston, 1998). Despite differences in isometric force production, maximum steady state or instantaneous power output in bass white muscle (~216 W kg⁻¹) is similar to values reported for these other fishes (e.g., ~189 W kg⁻¹ for sculpin, James et al., 1998).

4.2. Comparison with in vivo measurements

The result of *in vitro* estimates of power output during feeding strikes by largemouth bass support the validity of those recently reported by Carroll and Wainwright (2006). Particularly for the analysis of shortening limited to 12% under realistic activation patterns, there is a close match between the mean result of the modeling work (epaxial muscle estimated to produce ~69 W kg⁻¹) and the results of the present work (epaxial muscle estimated to produce 60–86 W kg⁻¹). This finding indicates that the model and methods used in the Carroll and Wainwright (2006) are broadly valid. The power produced by muscle bundles under the experimental velocity ramps is substantially less than the maximum steady state or instantaneous power (W_{max}) determined from the V_{max} experiments. During feeding strikes, muscle averages 28–40% W_{max} during the full range of shortening. However, the peak power produced during the experimental velocity ramps is closer to 60% of W_{max} .

Longer muscle strains led to lower power output in the *in vitro* velocity ramp experiments. The isolated muscle bundles began to relax after shortening by ~6% (Fig. 4), limiting power production during the full shortening period. However, in the *in vivo* measurements of Carroll and Wainwright, the epaxial muscle appears to generate relatively high force through at least 10% of muscle shortening (see Fig. 5, Carroll and Wainwright, 2006). This difference in part explains how *in vivo* estimates of epaxial muscle power output in some muscle strikes were substantially higher (i.e., up to 300 W kg⁻¹) than any measurements made *in vitro* though measurement error may account for some of this discrepancy. The difference in force production relative to level of strain also suggests that *in vitro* experimentation with isolated muscle bundles does affect the physiological properties of muscle.

It has been proposed by several authors that suction feeding muscles ought to function to produce mechanical power (Muller et al., 1982; Van Wassenbergh et al., 2005). To do so the musculoskeletal system must be constructed such that fascicles

may shorten at or near velocities that allow peak power production. Epaxial muscle shortens *in vivo* at about 32% of V_{\max} , close to the optimal shortening velocity observed in isolated muscle bundles (Fig. 3). The sternohyoideus muscle operates on average at a shortening velocity of approximately 2.5 ML s^{-1} during feeding strikes in bass (Carroll, 2004) which is about 19% of V_{\max} for this muscle. However, the fastest strikes approached $4\text{--}5 \text{ ML s}^{-1}$ which is consistent with muscle function for power production. The *in vitro* experiments suggest that the effect of shortening velocity on power output *in vivo* is relatively modest within the range of shortening velocities employed (Fig. 7). These findings indicate that in terms of shortening velocity, the epaxial and sternohyoideus feeding muscles operate at optimal muscle shortening velocity, at least for maximal feeding strikes. One important question is whether the optimal shortening velocities observed during feeding by bass are achieved across the morphological diversity found in teleost fish or whether musculoskeletal performance is compromised in some forms.

One of the goals of this research was to understand how the fluid mechanical environment influences the levels of power muscles are able to produce during suction feeding. It was found that the delay between onset of activation and onset of shortening *in vivo* was much shorter than that found to produce maximal power *in vitro* (Fig 6). The shorter latency *in vivo* is probably because as muscle force develops no pre-existing loads prevent the muscle from shortening (Wakeling and Johnston, 1999). While much attention has been given to organismal design for maximal power production during behaviors (e.g., Lutz and Rome, 1996b), or the design relationship between behavioral requirements and muscle functional parameters (Marsh, 1999), it appears that, at least during suction feeding, the lack of pre-existing loads precludes functional patterns that would result in maximal power.

Suction feeding in fishes requires the rapid generation of negative pressure within the buccal cavity to produce inward flows at the mouth opening. The epaxial musculature and, to a lesser extent, the sternohyoideus muscles power buccal cavity expansion and the generation of strongly negative pressures during feeding events in many fishes, including largemouth bass. Previous studies have used hydrodynamic modeling along with *in vivo* recordings of muscle length change and buccal pressure to estimate the power production by the epaxial muscle during a feeding strike in bass (e.g., Carroll and Wainwright, 2006). The present study used *in vitro* muscle mechanics experiments with isolated muscle bundles to quantify power production by a different means. In terms of estimates of mass specific power output by the epaxial musculature, the two techniques generated remarkably similar values. The present results support the conclusion of Carroll and Wainwright (2006) that the epaxial muscle produces the majority of power for suction feeding in bass. Further, the present research suggests that the epaxial musculature, although it is the primary source of power during suction feeding events by bass, operates in a sub-optimal manner, with a short latency between muscle activation and muscle shortening. This ultimately limits power output. We suggest that the need to maximize the speed of a feeding strike acts as a constraint on the efficient use of muscle to power that strike.

Acknowledgments

We thank Sean Dodson and Mahfuza Akhtar for laboratory assistance. This work was supported by funding from Widener University.

References

- Carroll, A.M., 2004. Muscle activation and strain during suction feeding in the largemouth bass *Micropterus salmoides*. *J. Exp. Biol.* 207, 983–991.
- Carroll, A.M., Wainwright, P.C., 2006. Muscle function and power output during suction feeding in largemouth bass, *Micropterus salmoides*. *Comp. Biochem. Physiol. A* 143, 389–399.
- Coughlin, D.J., 2000. Power production during steady swimming in largemouth bass and rainbow trout. *J. Exp. Biol.* 203, 617–629.
- Coughlin, D.J., Caputo, N.D., Bohnert, K.L., Weaver, F.E., 2005. Troponin T expression in trout red muscle correlates with muscle activation. *J. Exp. Biol.* 208, 409–417.
- Davies, M.L.F., Johnston, I.A., van de Wal, J., 1995. Muscle fibers in rostral and caudal myotomes of the Atlantic cod (*Gadus morhua*) have different mechanical properties. *Phys. Zool.* 68, 673–697.
- de Jong, M.C., Sparenberg, J.A., DeVries, J., 1987. Some aspects of hydrodynamics of suction feeding of fish. *Fluid Dyn. Res.* 2, 87–112.
- Ferry-Graham, L.A., Lauder, G.V., 2001. Aquatic prey capture in ray-finned fishes: A century of progress and new directions. *J. Morphol.* 248, 99–119.
- Ferry-Graham, L.A., Bolnick, D.I., Wainwright, P.C., 2002. Using functional morphology to examine the ecology and evolution of specialization. *Integr. Comput. Biol.* 42, 265–277.
- James, R.S., Cole, N.J., Davies, M.L.F., Johnston, I.A., 1998. Scaling of intrinsic contractile properties and myofibrillar protein composition of fast muscle in the fish *Myoxocephalus scorpius* L. *J. Exp. Biol.* 201, 901–912.
- Lauder, G.V., 1980. The suction feeding mechanism in sunfishes (*Lepomis*): An experimental analysis. *J. Exp. Biol.* 88, 49–72.
- Lauder, G.V., Lanyon, L.E., 1980. Functional anatomy of feeding in the bluegill sunfish, *Lepomis macrochirus*: *In vivo* measurement of bone strain. *J. Exp. Biol.* 84, 33–55.
- Lutz, G.J., Rome, L.C., 1996a. Muscle function during jumping in frogs. I. Sarcomere length change, EMG patter, and jumping performance. *Am. J. Physiol., Cell Physiol.* 271, C563–C570.
- Lutz, G.J., Rome, L.C., 1996b. Muscle function during jumping in frogs. II. Mechanical properties of muscle: Implications for system design. *Am. J. Physiol., Cell Physiol.* 271, C571–C578.
- Marsh, R.L., 1999. How muscles deal with real-world loads: The influence of length trajectory on muscle performance. *J. Exp. Biol.* 202, 3377–3385.
- Muller, M., Osse, J.W.M., Verhagen, J.H.G., 1982. A quantitative hydrodynamic model of suction feeding in fish. *J. Theor. Biol.* 95, 49–79.
- Reilly, S.M., Willey, J.S., Bikevicius, A.R., Blob, R.W., 2005. Hindlimb function in the alligator: Integrating movements, motor patterns, ground reaction forces and bone strain of terrestrial locomotion. *J. Exp. Biol.* 208, 993–1009.
- Roberts, T.J., Marsh, R.L., 2003. Probing the limits of muscle-powered accelerations: Lessons from jumping bullfrogs. *J. Exp. Biol.* 206, 2567–2580.
- Rome, L.C., Funke, R.P., Alexander, R.M., Lutz, G., Aldridge, H., Scott, F., Freadman, M., 1988. Why animals have different muscle fibre types. *Nature* 335, 824–827.
- Rome, L.C., Swank, D., Corda, D., 1993. How fish power swimming. *Science* 261, 340–343.
- Syme, D.A., Shadwick, R.E., 2002. Effects of longitudinal body position and swimming speed on mechanical power of deep red muscle from skipjack tuna (*Katsuwonus pelamis*). *J. Exp. Biol.* 205, 89–200.
- Van Wassenbergh, S., Herrell, A., Adriaens, D., Aerts, P., 2005. A test of mouth-opening and hyoid-depression mechanisms during prey capture in a catfish using high-speed cineradiography. *J. Exp. Biol.* 208, 4627–4639.
- Wakeling, J.M., Johnston, I.A., 1998. Muscle power output limits fast-start performance in fish. *J. Exp. Biol.* 201, 1505–1526.
- Westneat, M.W., 2004. Evolution of levers and linkages in the feeding mechanisms of fishes. *Integr. Comput. Biol.* 44, 379–389.